Roquin binds ICOS mRNA and effectors of mRNA decay to induce miRNA-independent post-transcriptional repression

Vigo Heissmeyer, Elke Glasmacher, Kai P Hoefig, Katharina U Vogel, Nicola Rath, Lirui Du, Christine Wolf, Elisabeth Kremmer, Xiaozhong Wang

Roquin binds *ICOS* mRNA and effectors of mRNA decay to induce miRNA-independent post-transcriptional repression

Elke Glasmacher[1], Kai P. Hoefig[1,3], Katharina U. Vogel[1,3], Nicola Rath[1], Lirui Du[1], Christine Wolf[1], Elisabeth Kremmer[1], Xiaozhong Wang[2] and Vigo Heissmeyer[1]*

[1] Helmholtz Zentrum München, German Research Center for Environmental Health, Institute of Molecular Immunology, Marchioninistr. 25, 81377 Munich, Germany.

[2] Department of Biochemistry, Molecular Biology and Cell Biology, Northwestern University, Evanston, Illinois 60208, USA.

[3] These authors contributed equally.

* Correspondence: vigo.heissmeyer@helmholtz-muenchen.de

Contact information

Vigo Heissmeyer, Ph.D.

Institute of Molecular Immunology

Helmholtz Center Munich

Marchioninistr. 25

81377 Munich, Germany

Phone + 49 89 7099 214

Fax + 49 89 7099 225

Abstract

The molecular mechanism by which Roquin controls the inducible T cell costimulator (ICOS) expression to prevent autoimmunity remains unsolved. Here we show that in helper T cells Roquin localized to processing (P) bodies and downregulated ICOS expression. The repression was dependent on Rck, and Roquin interacted with Rck and Edc4, which cooperate in mRNA decapping. Sequences in Roquin that confer P body localization were essential for Roquin-mediated ICOS repression. However, this process did not require microRNAs or the RNA-induced silencing complex. Instead, Roquin bound *ICOS* mRNA directly, exhibiting an intrinsic preference for a previously unrecognized sequence in the 3' untranslated region (3'UTR). Our results support a model in which Roquin controls ICOS expression through binding to the 3'UTR of *ICOS* mRNA and by interacting with proteins that confer post-transcriptional repression.

Introduction

Roquin is a CCCH-type zinc finger protein that destabilizes the mRNA of the inducible T cell costimulator (ICOS) in a process that requires the 3' untranslated region (3'UTR) of *ICOS* mRNA [1]. Loss of this post-transcriptional regulation causes autoimmunity in *Rc3h1*$^{san/san}$ mice, which are homozygous for a point mutation in the *Rc3h1* gene that encodes Roquin [1,2]. How *ICOS* mRNA is recognized by Roquin protein and how this recognition induces mRNA decay is currently unknown.

Post-transcriptional regulation of gene expression controls key decisions of innate and adaptive immune responses [3-5]. Pathways involved in translational repression and mRNA decay employ many different molecular mechanisms, but uniformly depend on trans-acting factors that bind to *cis*-regulatory elements within target mRNAs. One class of trans-acting factors are miRNAs that, when loaded onto the RNA-induced silencing complex (RISC), can base pair with partially complementary sequences in the 3'UTR of target mRNAs [5]. RNA-binding proteins represent another class of trans-acting factors. *Cis*-elements for these factors have been described within single-stranded RNA, however they are not well-defined, and the recognition is thought to depend on shape as well as sequence [3,6]. Trans-acting RNA-binding proteins and miRNAs can target the same mRNA. The different trans-acting factors can either cooperatively repress the target [7], or the RNA-binding protein can block miRNA-dependent repression [8]. In addition, trans-acting protein factors cooperate with miRNAs and argonaute (AGO) proteins in an opposing program and augment translation [9]. Whether the different pathways of post-transcriptional regulation cooperate in general or work in parallel and converge under specific cellular conditions needs further investigation and requires a genetic dissection of the involved molecules.

A 3'UTR region of *ICOS* mRNA was recently described as important for Roquin-mediated ICOS repression [1]. Based on the investigation of a putative miR-101 binding site within this region, a functional dependence of Roquin on miRNAs has been suggested [1]. However, it remains unclear whether the miRNA itself or a

Roquin-miRNA or -miRISC complex is the trans-acting factor that enables recognition of the mRNA and repression of cellular ICOS levels.

ICOS expression is strongly induced on the surface of T cells after recognition of antigen. Its transcription is upregulated early after T cell receptor (TCR) triggering and in response to NFAT activation. However, highest ICOS protein levels appear with a temporal delay, demonstrating pronounced post-transcriptional regulation [10]. The induced ICOS expression regulates cytokine production in T cells allowing them to provide B cells help for high affinity antibody production in the germinal center reaction [11-15].

Rc3h1$^{san/san}$ mice that express mutated Roquin proteins show spontaneous germinal center formation and develop autoimmune phenotypes that are similar to the disease systemic lupus erythematosus in human patients [2]. Consistent with their aberrant high ICOS expression in T cells, these mice have increased numbers of follicular helper T cells [1,2,16]. However, several autoimmunity-associated phenotypes disappear in *Rc3h1*$^{san/san}$ mice that are heterozygous for *Icos* gene deficiency [1], indicating that ICOS is the critical target in Roquin-mediated prevention of lupus-like autoimmunity. The *Rc3h1*$^{san/san}$ mutation is positioned in the ROQ domain of Roquin and renders it less effective in controlling ICOS expression [1]. The integrity of the ROQ domain is therefore essential in the prevention of autoimmunity, however the molecular function of this domain remains unclear.

Here, we show that Roquin is the trans-acting factor that targets *ICOS* mRNA for post-transcriptional repression. Roquin binds RNA through its ROQ domain and CCCH-type zinc finger and recognizes a region in the 3'UTR of *ICOS*. Roquin also interacts with processing (P) body factors, which are involved in mRNA decay, and is able to repress ICOS even in the complete absence of cellular miRNAs or RISC formation.

Results

ICOS expression is controlled by Roquin

To investigate the contribution of Roquin to ICOS regulation in differentiated helper T (T_H) cells we established an adenoviral knockdown approach. Primary $CD4^+$ T cells from *Tg(DO11.10) Tg(CARΔ-1)* mice were used to introduce adenoviral expression vectors [17]. T cells from these mice are permissive for adenoviral infection through transgenic expression of a signaling-inactive version of the human coxsackie adenovirus receptor (CARΔ-1). Infection of $CD4^+$ T cells was performed prior to activation with anti-CD3 and anti-CD28 antibodies in culture conditions that skew helper T cell differentiation. By expression of adenoviral vectors coexpressing GFP with shRNAs against the Roquin-encoding gene *Rc3h1* or the control *Cd4* gene, we were able to downregulate protein (**Fig. 1a,b**) and mRNA expression (**Fig. 1c,g**). However, downregulation of the Roquin protein was only observed in the highest (10-25%) GFP-expressing cells, correlating with the observed lower efficiency of RNA interference in primary CD4 T cells [18]. Knockdown of Roquin increased ICOS protein and mRNA levels in T_H0, T_H1 and T_H2 cells (**Fig. 1b-f**). The effect was specific, because it did not affect CD4 protein expression (**Fig. 1b**, lower panel) or mRNA expression of *Rc3h2* (**Fig. 1c**), the paralog of Roquin [19]. In addition, ICOS expression was not induced by expression of an empty shRNA vector or by knockdown of CD4 (**Fig. 1b**, upper panel). Quantification of ICOS protein surface expression (**Fig. 1d,e**) and *ICOS* mRNA (**Fig. 1f**) during activation and differentiation of CD4 T cells under T_H0, T_H1 and T_H2 conditions demonstrate that ICOS protein and mRNA amounts increase from T_H0 to T_H1 to T_H2 (**Fig. 1d-f**), as previously reported [10]. Irrespective of the differentiation conditions, a significant increase of ICOS surface levels (**Fig. 1d,e**) occurred in sh-*Rc3h1* transduced cells. A similar increase of *Icos* mRNA was observed in the bulk population containing 72-90% GFP positive cells (**Fig. 1f**). The knockdown reduced *Rc3h1* mRNA to 46-75% of endogenous levels in the bulk population (**Fig. 1g**). These findings show that the expression of ICOS is placed under post-transcriptional control of Roquin in helper T cells.

Roquin interacts with the P body pathway

We employed deletion mutagenesis to identify regions in the Roquin protein that are critical for the repression. The mutants were analyzed in mouse embryonic fibroblast (MEF) cells that were first transduced with full-length human *ICOS* mRNA expressing retroviruses and subsequently superinfected with IRES–Thy-1.1 retroviruses encoding wild-type or mutant versions of Roquin. Truncation of the 3' end of the coding region in mutant Roquin(1–509), which lacks the proline-rich and the coiled-coil regions, inactivated Roquin-mediated ICOS repression (**Fig. 2a-c**). In contrast, Roquin(1–951), a mutant lacking only the carboxyterminal coiled-coil domain, was slightly less active compared to the wild-type (**Fig. 2a-c**).

The inactive Roquin(1–509) mutant fused to GFP displayed aberrant diffuse cytoplasmic localization upon transfection into HEK293 cells (**Supplementary Fig. 1a**, lower panel), in contrast to the localization of Roquin(1–951) and wild-type Roquin–GFP fusion proteins. These proteins localized to cytoplasmic foci and exhibited little diffuse cytoplasmic stain (**Supplementary Fig. 1a**, upper panel). We tested Roquin localization in GFP–Roquin transduced primary $CD4^+$ T cells (**Fig. 2d**) and transfected HEK293 cells (**Supplementary Fig. 1b**) by co-staining with antibodies that robustly identify P bodies or stress granules. Many of the Roquin-enriched foci in HEK293 or $CD4^+$ T cells showed full co-localization with Rck protein, and were therefore identified as P bodies [20]. In contrast, FMRP, a marker protein of stress granules [21,22], showed a diffuse stain in both cell types in the presence or absence of ectopic Roquin expression (**Fig. 2d**, upper panel and **Supplementary Fig. 1b**, upper panel). Consistently, anti-G3BP1 staining confirmed the absence of stress granules in $CD4^+$ T cells upon expression of Roquin (**Supplementary Fig. 1c**, upper panel). Quantification of GFP–Roquin localization in $CD4^+$ T cells showed that in 62% of cells Roquin was associated with P bodies, whereas localization to the stress granules was found in only 1.7% of the cells. There was no effect of Roquin expression on the percentage of cells

having P bodies (i.e. 68% of all cells) or having stress granules (i.e. 18% of all cells) or on the number of P bodies and stress granules per cell (data not shown).

Subjecting $CD4^+$ T cells to arsenite-induced stress (**Fig. 2d**, lower panel) induced stress granule formation in 85% of cells and 89% of GFP–Roquin expressing cells showed an association of Roquin with stress granules. In only 5.5% of these cells Roquin remained associated with P bodies. Experimental stress induction did neither change the percentage of cells that were positive for P bodies nor the number of P bodies (i.e. on average 2) or stress granules (i.e. on average 2.75 granules) per cell (data not shown). Similarly, in HEK293 cells the colocalization of Roquin and Rck was nearly completely abrogated when cells were treated with arsenite to induce oxidative stress (**Supplementary Fig.1b**, lower panel). During aggregation of messenger ribonucleoprotein (mRNP) complexes that form P bodies, glutamine and asparagine (Q and N)-rich sequences mediate protein-protein interactions [23-25]. The carboxyterminal region of Roquin revealed an increased frequency of Q and N residues in sequences adjacent to the proline-rich region [25]. Artificially defined frames of 80 amino acids reach a maximum content of 17 Q and N residues in mouse Roquin, with 7.68 as the predicted average [25]. We therefore investigated localization and function of a mutant, Roquin(1–749), that contains the proline-rich region, but lacks the sequences enriched in Q and N residues. This mutant had impaired foci formation in the absence of stress (**Fig. 3a**, upper panel), but was still able to translocate into stress granules upon arsenite treatment (**Fig. 3a**, lower panel). Overexpression of this mutant interfered with P body formation, as judged from a diffuse cytoplasmic localization of Rck (**Fig. 3a**, upper panel). However, after induction of stress, the Rck-labeled foci quickly reappeared (**Fig. 3a**, lower panel). In functional assays, the mutant protein Roquin(1–749) was strongly impaired in ICOS downregulation after sequential infection of the mouse fibroblast cell line NIH3T3 (**Fig. 3b,c**). These findings positively correlate Roquin function with its localization to P bodies, but not to stress granules.

To investigate the possibility that stress granules are dispensable, we tested Roquin function in the absence of T cell intracellular antigen-1 (TIA-1) (**Supplementary Fig. 2c**). TIA-1-deficient MEF cells have impaired stress granule assembly as determined by TIAR, G3BP and eIF3 staining [26]. In TIA-1-deficient and control MEF cells (**Fig. 3d**) sequentially transduced with retroviral ICOS and Roquin constructs, there was virtually no effect of *Tia1* gene deletion on the ability of Roquin to repress ICOS levels (**Fig. 3d,e**). The data suggest that, at least in the absence of cell stress, Roquin-mediated ICOS repression does not depend on TIA-1 function, requiring instead physical or functional interactions with P body components.

Roquin interacts with decapping proteins

To identify Roquin-interacting proteins, we generated a rat monoclonal antibody directed against an internal peptide of Roquin (**Supplementary Fig. 2 a,b**). By mass spectrometry, we identified the helicase Rck, the enhancer of decapping Edc4 and the decapping activator Dcp1a in T_H1 extracts immunoprecipitated with the Roquin purified antibody coupled to magnetic beads, but not in control precipitations (beads coupled to an irrelevant antibody, data not shown). We confirmed that Edc4 as well as the helicase Rck, another essential component of the decapping pathway, were associated with immunoprecipitated Roquin protein in T_H1 (**Fig. 4a**) and in MEF cells (**Fig. 4b**). Edc4 interacted more strongly compared to Rck, because the protein appeared enriched in immunoprecipitation over the input levels. Rck was significantly and specifically associated, but was not enriched in anti-Roquin immunoprecipitations compared to input levels. GFP–Roquin(1–509) also interacted with endogenous Edc4 in anti-GFP immunoprecipitates from adenovirus-transduced MEF cell extracts (**Fig. 4c**). The interaction occurred through aminoterminal sequences in Roquin, did not require localization of Roquin to P bodies (**Fig. 3a** and **Supplementary Fig. 1a**) and was insensitive to an RNase treatment during the immunoprecipitation procedure that efficiently degraded the 28S and 18S rRNA in RNA extracts prepared from

immunoprecipitation supernatants (**Fig. 4c**, lower panel and data not shown). Consistent with a possible association of all three proteins in one complex we observed the full colocalization of Edc4, Rck and GFP–Roquin in HEK293 cells in the absence of stress induction (**Supplementary Fig. 2d**).

Decreasing cellular Rck levels in ICOS and Roquin IRES–Thy-1.1 retrovirally transduced MEF cells led to very effective de-repression of ICOS (**Fig. 4e,f**). Knockdown was obtained by superinfection with adenoviruses that encode an shRNA against *Rck* (**Fig. 4d**) and ICOS expression was higher than before Roquin transduction (**Fig. 4e,f**). This experiment indicated that Rck knockdown neutralized the function of exogenous as well as of endogenous Roquin protein, which is detectable in MEF cells (data not shown). These data are consistent with a model in which Roquin mediates silencing of ICOS through functional and physical interaction with proteins of the decapping pathway.

MiRNAs are not required for Roquin-mediated repression

The Rck protein is not only required in the decapping pathway, but is also essential in miRNA-dependent post-transcriptional silencing [20]. This pathway has previously been implicated in Roquin-mediated ICOS repression [1]. We generated Dicer-deficient MEF clones by transduction of *Dicer1*$^{fl/fl}$ and wild-type cells with Cre-recombinase expressing retroviruses. In parallel, we used CD4$^+$ T cells from *Dicer1*$^{fl/fl}$ *CD4-Cre* and *Dicer1*$^{+/fl}$ *CD4-Cre* mice. Real-time PCR for several candidates and global high-throughput sequencing of small RNAs revealed almost undetectable levels of miRNAs in Dicer-deficient MEF clones (**Supplementary Fig. 3a,b** and [27]). In contrast, although peripheral CD4$^+$ T cells from *Dicer1*$^{fl/fl}$ *CD4-Cre* mice showed efficient deletion of the targeted alleles (**Supplementary Fig. 3c**), detectable miRNA expression varied between 20-60% of the endogenous levels of miR-101, miR-155 and miR-181 (**Supplementary Fig. 3d**). These findings suggest a very long half-life of RISC-loaded miRNAs during T cell development and, at the same time, rule out the possibility of testing a miRNA-requirement in Roquin-mediated ICOS expression in CD4$^+$ T cells.

Wild-type and Dicer-deficient MEF cells were therefore infected with retroviruses encoding ICOS and Roquin, or with ICOS and Roquin(1–509) (**Fig. 5a,b**). Wild-type Roquin, unlike its inactive mutant, efficiently downregulated ICOS surface expression in wild-type and in Dicer-deficient cells (**Fig. 5a,b**). Moreover, Roquin-mediated repression of ICOS levels occurred in wild-type and in Dicer- and miRNA-deficient cells with a similar dose response, as evident from quantification of ICOS levels on cells with low, intermediate or high surface expression of Thy-1.1, the marker coexpressed by the Roquin-encoding retrovirus (**Fig. 5c**). In addition, Roquin induced a similar decrease of *ICOS* mRNA expression in wild-type and Dicer-deficient cells (**Fig. 5d**). Wild-type and Roquin(1–509) protein expression was equally efficient in wild-type and Dicer-deficient cells (**Supplementary Fig. 3e**, compare lane 1 with 4 and lane 2 with 3). We did not detect increased expression of endogenous Roquin protein (**Supplementary Fig. 3e**, compare lane 1 and 4 and **Supplementary Fig. 3f**) or *Rc3h1* mRNA (data not shown) in cells with deletion of Dicer.

We also performed functional tests on Dicer-deficient cells and measured miR-196a-induced translational repression of the *Hoxc8* 3'UTR, a well-established target of this miRNA [28]. We found that the *Hoxc8* 3'UTR was strongly repressed by coexpression of a construct encoding pri-miR-196a in wild-type, but not in Dicer-deficient cells (**Fig. 5e**). In contrast, the Dicer-deficient cells that were impaired in miRNA-biogenesis and gene silencing were still able to support Roquin-mediated repression of a luciferase reporter through the 3'UTR of *ICOS* mRNA (**Fig. 5e**). We next asked whether Roquin has to cooperate with central components of the RISC to induce repression of ICOS. We tested Roquin-induced downregulation of the *ICOS* 3'UTR in embryonic stem (ES) cells that are homozygous for a deletion of *Ago1*, *3* and *4* (line B9) [29]. We also analyzed ES cells (line E7) deficient for endogenous mouse *Ago1-4* gene products, but can still be expanded in culture due to low expression of a human *AGO2* transgene from a loxP-flanked locus. In these cells, human *AGO2* can be ablated by virtue of an estrogen receptor-fused Cre recombinase, induced by tamoxifen treatment (line E7 with 4'OH-T). After tamoxifen treatment these cells remain viable for up

to four days before undergoing apoptosis [29]. Coinfection of GFP or Roquin IRES–GFP with the *ICOS* 3'UTR reporter construct (**Fig. 5f**) revealed that Roquin was able to repress the *ICOS* 3'UTR in cells lacking mouse Ago1, 3 and 4 (line B9) and in cells that lack mouse Ago1-4, but contain low amounts of human AGO2 (line E7). After 4'OH-T treatment, E7 cells were arrested in proliferation, but were not impaired in Roquin-mediated ICOS repression, as determined by luciferase measurements (**Fig. 5f**) or FACS analysis (data not shown). The ratio between renilla luciferase activity and firefly luciferase activity gives a measurement of *ICOS* 3'UTR-mediated repression of renilla luciferase expression. This is independent of infection efficiency, epigenetic regulation of the adenoviral episomes and relative transcription or translation efficiencies in different cell types. Comparing these normalized values, we did not find evidence that repression of the *ICOS* 3'UTR changed upon partial or complete inactivation of miRISC function. Therefore, we did not detect regulation of the *ICOS* 3'UTR through miRNAs in ES cells (**Fig. 5f**). However, we cannot exclude miRNA-dependent regulation of ICOS in other cell types. In fact, we measured *ICOS* mRNA expression normalized to *Hprt1* from retroviruses that integrated into the genome of Dicer-deficient and wild-type MEF cells (**Supplementary Fig. 3g**) and compared this expression to the amount of PCR amplification of the retroviral vector encoded GFP sequence normalized to the *Hist1h2ak* gene (**Supplementary Fig. 3h**). We found a modestly increased ICOS expression per integration in Dicer-deficient cells (**Supplementary Fig. 3i**) suggesting a moderate repressive effect of miRNAs on the *ICOS* 3'UTR in MEF cells.
Together, these findings cannot exclude cell-type specific regulation of ICOS by miRNAs, but rule out a requirement for miRNAs and RISC formation in Roquin-mediated ICOS repression.

Roquin is an RNA-binding protein

We next tested whether Roquin itself interacts with mRNA. First, we addressed whether we could detect endogenous mouse *Icos* mRNA in endogenous Roquin

immunoprecipitates from primary T_H1 cell protein extracts. We documented efficient Roquin protein enrichment (**Fig. 6a**) in immunoprecipitates and confirmed physical association of *Icos* mRNA and Roquin protein by showing significant *Icos* PCR-amplification in the Roquin immunoprecipitations compared to mock precipitations in three independent experiments (**Fig. 6b**). The observed interaction did not depend on the carboxy- but on the aminoterminus of Roquin. In fact, interaction of Roquin and *ICOS* mRNA after cotransfection in HEK293 cells was equal or moderately increased in the Roquin(1–509) mutant (**Fig. 6c**). Deletion of the aminoterminal RING finger alone, in Roquin(55–1130), had a small negative effect on the interaction with *ICOS* mRNA (**Fig. 6c**). However, *ICOS* mRNA binding was lost when the aminoterminal deletion in the Roquin(338–1130) mutant included the ROQ domain (**Fig. 6c**). Roquin-mediated repression of ICOS was completely abolished when the RING finger and ROQ domain were deleted in Roquin(338–1130), whereas deletion of the RING finger alone in Roquin(55–1130) had a partial effect (**Fig. 6d,e**). Finally, to address a possible contribution of the CCCH-type zinc finger, we expressed a truncated Roquin protein, Roquin(1–412), that contained the RING finger and ROQ domain, but lacked the carboxyterminal sequences including the zinc finger. This mutant showed a strong impairment in *ICOS* mRNA binding, however it was found associated with more *ICOS* mRNA than in control immunoprecipitates (**Fig. 6f**). These findings show that the zinc finger cooperates with the ROQ domain, which is critical in the binding to *ICOS* mRNA.

Finally, we investigated whether Roquin, in the absence of other cellular factors, was able to bind and recognize *ICOS* mRNA. We bacterially expressed and purified an aminoterminal fragment of the protein, Roquin(1–441), that contained the RING finger, ROQ and zinc finger domains (**Supplementary Fig. 4a**). We incubated the protein with capped full-length *ICOS* mRNA that was generated by T7 polymerase *in vitro* transcription (**Supplementary Fig. 4b**). In electromobility shift assays (EMSA) Roquin protein interacted with full-length *ICOS* mRNA (**Fig. 7a**), and the Roquin-induced retardation of the *ICOS* mRNA band was increased at higher Roquin concentrations in the binding reaction (**Fig. 7a**, lanes 2-8). The

progressive upshift increased over a wide range of protein concentrations (**Fig. 7a**, lane 4-8), indicating the existence of several or many binding sites for Roquin on the *ICOS* mRNA.

ICOS mRNA expression from a construct lacking the 3'UTR was not repressed in cells overexpressing Roquin [1]. Consistent with this finding, we did not detect any regulation of *ICOS* mRNA by Roquin when the 3'UTR of *ICOS* was replaced with an unrelated 3'UTR (data not shown) or with a non-responsive sequence, that is, a second coding sequence of *ICOS* without start and stop codons (**Supplementary Fig. 5a**, lower panel). Only the full-length *ICOS* harboring the 3'UTR was efficiently bound by Roquin *in vitro*, whereas the *ICOS* coding sequence (CDS) (**Fig. 7a**, lanes 10-16) or tandem coding sequences of *ICOS* (CDS-CDS) (**Supplementary Fig. 5b**) were not well recognized and not shifted by Roquin at low protein concentrations (**Supplementary Fig. 5b**, compare lane 2-5 with 7-10 and 12-15). Furthermore, Roquin did not shift excess yeast transfer RNA that was included in the binding reaction (**Supplementary Fig. 4c**) and under these conditions an unrelated protein did not induce retardation of the full-length *ICOS* mRNA band (**Supplementary Fig. 4d**). The binding was not due to the T7 terminator sequence (**Supplementary Fig. 4e,f**) or dependent on the attachment of a poly(A)-tail (data not shown). However, at high protein concentrations the coding sequence could also be shifted by Roquin protein. We therefore quantified the effective Roquin protein concentration that was required for complete binding of different constructs as determined by disappearance of the free mRNA. A full upshift of the free *ICOS* full-length mRNA was already observed at 20 pmol whereas the complete upshift of *ICOS* CDS mRNA was not observed below 160 pmol of Roquin protein per binding reaction, indicating an approximately 8-fold difference in Roquin affinity for the two different mRNAs (**Fig. 7a**, lanes 2 and 15). We mapped the site that was required for the higher affinity binding within the 3'UTR of *ICOS* by introducing progressive 600 bp deletions starting from the 3'end. An *ICOS* 3'UTR mRNA construct (1–1210), containing the coding sequence and the first 600 bp of the 3'UTR responded to Roquin binding indistinguishable from full-length *ICOS* (**Supplementary Fig. 6a**).

Roquin(1–441) bound this minimal *ICOS* 3'UTR (1–1210) construct with higher affinity, compared to an irrelevant mRNA of similar length (the coding sequence of the human *FOXP3* gene, **Supplementary Fig. 6b**). By removing in a stepwise manner 100 bp from the 3'end of this *ICOS* construct (**Fig. 7b**), we identified the region between 100 and 200 bp 3' to the stop codon as critical for the higher affinity binding of Roquin to the *ICOS* 3'UTR. We also correlated the sequences that are required for the higher affinity binding of *ICOS* mRNA by Roquin with the extent of functional repression of ICOS by Roquin in MEF cells (**Fig. 7c,d**). All constructs containing the mapped binding site were repressed by Roquin. However, the degree of ICOS repression by Roquin increased with length of the *ICOS* 3'UTR. These findings indicate that multiple sites within the 3'UTR may actually contribute to the functional repression of ICOS by Roquin in living cells.

Discussion

Our data strongly involve P body components in Roquin-mediated ICOS repression. We show that localization of Roquin to P bodies occurs in primary $CD4^+$ T cells as well as in HEK293 cells and could be equally detected by colocalization with Rck and Edc4, two different P body markers. In fact, in HEK293 or $CD4^+$ T cells not subjected to stress, we did not find colocalization of Roquin-enriched foci with the stress granule markers FMRP or G3BP1. The localization to P bodies requires the carboxyterminus of Roquin that contains Q and N-enriched sequences. Glutamine stretches were shown to act as polar zippers in prion proteins [24] and an increased content of Q and N-residues was also determined in many P body proteins. These regions are believed to permit protein-protein interactions important for mRNP formation in post-transcriptional regulation [23,25]. The presence and the functional importance of sequences that are Q and N-enriched provide support for an evolutionary conserved role of Roquin in the P body pathway. In relation to the previously reported localization of Roquin to stress granules [2,30], we noticed that Roquin can translocate into stress granules upon induction of stress in HEK293 and $CD4^+$ T cells and it is

therefore possible that cells undergoing a stress response have altered Roquin-activity. So far, we have not been able to obtain experimental support for this notion. We show that Roquin effectively represses ICOS levels in helper T cells, in a phase in which the TIA-1-dependent integrated stress response was shown to repress translation of *IL-4* mRNA [31]. However, we did not observe any effect on Roquin activity in MEF cells deficient for TIA-1. Within the P body pathway, we have identified binding of Roquin to the P body components Edc4 and Rck in $CD4^+$ T cells and MEF cells and have demonstrated the importance of Rck expression for Roquin function. Rck and Edc4 operate in the decapping pathway and destabilize mRNAs in a functional cooperation with Dcp1a and Dcp2, the latter of which removes the 5' N7-methylguanosine (^{m7}G) cap. The mRNAs that lack this modification are no longer protected from 5' to 3' mRNA degradation [23]. Nevertheless, the repression of mRNA translation by interfering with binding of the translation initiation factor complex eIF4F to the (^{m7}G) cap of the mRNA represents the rate-limiting step of decapping [32-34]. Therefore, while not excluding a role for Roquin in the first step of translational repression, our results propose that Roquin promotes decapping of target mRNAs.

We also present evidence that Roquin is an RNA binding protein. The observed association of Roquin and *ICOS* mRNA in T cell extracts or cell extracts from transfected HEK293 cells primarily depended on the ROQ domain, showing that this domain is a member of a relatively small group of RNA-binding modules [35]. It appears that the ROQ domain binds in combination with the CCCH-type zinc finger module in Roquin. This mode of protein-RNA interaction allowed binding of multiple Roquin molecules to the same *ICOS* mRNA *in vitro*. The cooperation of different RNA-binding modules within one protein has been described as a common feature of RNA-binding proteins and typically enables them to bind with higher affinity or to obtain specificity for an mRNA substrate within an enormous diversity of possible structures [35]. These findings are consistent with a very recent report, which also demonstrated that the ROQ domain is critical for binding of Roquin to a short RNA-fragment from the *ICOS* 3'UTR [30]. However, we find that Roquin prefers certain structure or sequence determinants present in a

previously unrecognized region of the *ICOS* mRNA, which are likely to specify the cellular targets of Roquin. Our experiments reveal the higher binding affinity of Roquin to a specific sequence that is located between 100 and 200 bp downstream of the stop codon in the *ICOS* 3'UTR. In addition, we find general binding to different mRNAs with a lower affinity, involving the possibility that sequential binding on the *ICOS* mRNA could occur in a cooperative manner. We conclude that Roquin is a protein that binds mRNAs with lower affinity. However, Roquin has a protein-intrinsic higher affinity for sequence or structure determinants of the *ICOS* 3'UTR. The fact that the *ICOS* 3'UTR contributes more regulatory elements than just one single Roquin-specific binding site for efficient repression of ICOS levels in cells implicates additional steps beyond binding. Therefore, we propose that the repression occurs in a higher order structure that is induced by Roquin recognition of the *ICOS* 3'UTR, but at the same time requires cellular co-factors which may require additional features in the *ICOS* 3'UTR.

We have analyzed Roquin activity in Dicer- and AGO1-4-deficient cells. We did not find evidence for a positive role of the miRISC as was previously suggested by studies describing that silencing of ICOS by Roquin required an intact miR-101 recognition motif [1]. In these experiments, a critical region in the 3'UTR of *ICOS* was mapped, and a minimal response element of 47 bp was defined [1]. We assume that experimental differences related to using isolated fragments linked to reporters or, in our case, the entire 3'UTR in the context of the *ICOS* coding sequence, may account for the contrasting conclusions.

The newly described molecular functions of Roquin may play a role in prevention of autoimmunity. These functions include the sequence or structure-specific binding to RNA as well as the complex formation with other factors that are involved in mRNA decay. We speculate that at least one of these functions could be impaired in Roquin proteins that harbor the M199R mutation in the ROQ domain and thereby cause the development of autoimmune disease in *Rc3h1*$^{san/san}$ mice [2].

Acknowledgements

We like to thank M. Schmidt-Supprian (Max Planck Institute for Biochemistry Martinsried, Germany) and D. Niessing (Helmholtz Zentrum München, Munich Germany) for critical reading of the manuscript and helpful discussions. We also thank C. Vinuesa (The John Curtin School of Medical Research, Canberra, Australia) for providing ICOS and Roquin cDNAs and G. Hannon for Dicer1$^{fl/fl}$ mice, N. Kedersha and P. Anderson (Brigham and Womens Hospital, HMS, Boston, USA) for TIA-1 knockout MEFs and U. Fischer (Biozentrum Würzburg, Germany) for the anti-FMRP antibody. We thank H. Sarioglu (Helmholtz Zentrum München, Munich Germany) for the mass spectrometry analysis and C. Thirion and L. Behrend (Sirion Biotech, Martinsried, Germany) for advice and reagents for adenoviral infections. This work was supported by grants of the Deutsche Forschungsgemeinschaft (SFB 571) and by the Fritz Thyssen Stiftung to VH.

Figure Legends

Figure 1. ICOS expression is placed under the control of Roquin in differentiated helper T cells. (a) Immunoblot of Roquin protein expression in FACS sorted CD4$^+$ T cells from DO11.10 CARΔ1 mice infected with sh-*Rc3h1* adenoviral vectors and stimulated with plate bound anti-CD3-CD28 antibodies under T_H0 conditions. (**b**) ICOS or CD4 protein expression in cells transduced with vectors encoding sh-control, sh-*Rc3h1* or sh-*Cd4* and stimulated under T_H2 conditions. (**c**) RT-PCR of mRNA expression for *Icos*, *Rc3h2* and *Rc3h1* in the highest (10%) fraction of GFP expressing cells sorted from sh-*Rc3h1* or sh-control transduced cells stimulated under T_H1 conditions (p=0.001 (two asterisks) and p=0.002 (one asterisk)). (**d,e**) One representative plot (**d**) or the average mean fluorescence intensity from three independent experiments (**e**) of ICOS

protein expression in gated GFP positive cells infected with adenoviral sh-*Rc3h1* and sh-control vectors stimulated with anti-CD3-CD28 under the indicated conditions is shown (p=0.035 (T_H0), p=0.023 (T_H1) and p=0.029 (T_H2)). (**f,g**) RT-PCR of *Icos* (**f**) and *Rc3h1* (**g**) mRNA expression in the bulk population of sh-*Rc3h1* or sh-control transduced cells containing 72-90% GFP^+ cells after stimulation with anti-CD3-CD28 under the indicated conditions. One representative analysis out of three is shown in (**a,b,c,d,f,g**).

Figure 2. Carboxyterminal sequences in Roquin are required for ICOS repression and Roquin localization. (**a**) Schematic representation of the domain organization of Roquin, depicting the RING finger (RING), ROQ domain (ROQ), zinc finger (Zinc), a region of high proline content (Proline-rich) and the coiled-coil domain (Coiled-coil). Numbers indicate the amino acid positions that were used as amino- or carboxyterminal ends of deletion mutants. (**b**) Representative plots of ICOS and Roquin (as Thy-1.1) expression. (**c**) Mean fluorescence intensity of ICOS, normalized in all samples within one experiment to ICOS expression in the control (Thy-1.1 empty vector, set to 100%). The graph represents the summary of the three independent experiments with the bars showing the average of ICOS mean fluorescence and the error bar indicating the standard deviation (p=0.027 (asterisk) and p=0.008 (bold asterisk)). (**d**) Confocal microscopy showing Rck (blue) and FMRP (red) colocalization with GFP-tagged wild-type Roquin (green), with and without arsenite treatment in primary $CD4^+$ T cells after 48 h of plate bound anti-CD3-CD28 stimulation. Enlarged view (Zoom) and individual white arrows identify representative Rck-, GFP- and FMRP-labeled foci in the pictures from individual channels or in the overlay.

Figure 3. Roquin-mediated ICOS repression correlates with P body localization, independently of the stress granule factor TIA-1. (**a**) Confocal microscopy showing Rck (blue) and FMRP (red) colocalization with the GFP-

tagged mutant Roquin(1–749) (green), with and without arsenite treatment in HEK293 cells. White boxes indicate the areas shown in the enlarged view (Zoom) and individual white arrows identify representative Rck-, GFP- and FMRP-labeled foci in the pictures from individual channels or in the overlay. (**b-e**) Representative plots of ICOS and Roquin (as Thy-1.1) expression. In three independent experiments with NIH3T3 cells (**b,c**) or wild-type and TIA-1-deficient MEFs (**d,e**) ICOS levels were analyzed as above (**Fig. 2b,c**). The Roquin(1–749) and Roquin(WT) protein expressing cells showed a significant difference in ICOS mean fluorescence intensity (**c**, p=0.006 (asterisk)), whereas in TIA-1-deficient and wild-type cells ICOS mean fluorescence intensity was similar (**e,** p=0.07 (NS)).

Figure 4. Roquin protein is associated with Rck and Edc4 and shows functional dependence on Rck expression. (**a,b**) Immunoprecipitations (Ppt) of protein extracts from cultured T_H1 cells (**a**) or MEF cells (**b**) with monoclonal anti-Roquin antibody coupled to magnetic beads. The control included beads coupled to an irrelevant antibody (**a**) or an isotype control (**b**). (**c**) Immunoprecipitations of protein extracts from MEF cells with polyclonal anti-GFP antibodies. Cells overexpressed (overexp) the indicated GFP-tagged deletion mutant of Roquin or GFP. RNase treatment (+RNase) was controlled with ethidium bromide (EtBr) staining. (**d-f**) Knockdown of *Rck* in MEF cells transduced with retroviruses encoding ICOS and the indicated Roquin proteins and superinfected with adenoviruses encoding shRNAs against *Rck* or control shRNA constructs (sh-control, sh-scrambled=sh-scr). (**d**) Western blot analysis of Rck protein expression levels. (**e,f**) Representative plot (**e**) and ICOS expression levels (**f**) in cells that were transduced with Roquin and superinfected with sh-*Rck*. The bar diagram shows the average mean fluorescence intensity of three independent experiments (p=0.034 (asterisk)).

Figure 5. Roquin-mediated ICOS repression does not depend on miRNAs or miRISC formation. (**a-d**) Representative plot of ICOS and Roquin (as Thy-1.1)

expression (**a**), mean fluorescence of ICOS expression (**b,c**) and *ICOS* mRNA levels (**d**) in one representative (**a,d**) or as an average of three independent experiments (**b,c**) in *Dicer1*$^{-/-}$ and wild-type MEF cells transduced with retroviruses to coexpress ICOS and the indicated Roquin proteins (**b**, p=0.046 (asterisk)). ICOS levels were analyzed as above (**Fig. 2b,c**). (**c**) ICOS levels on cells with low (Lo), intermediate (Int) or high (Hi) surface expression of Thy-1.1 are compared to cells with low Thy-1.1 levels. (**e,f**) Luciferase activity in wild-type and *Dicer1*$^{-/-}$ MEF cells (**e**) and in the ES cell lines B9 and E7 (**f**). The luciferase activity is the ratio of renilla luciferase units to firefly luciferase units. The *Hoxc8* or *ICOS* 3'UTR (as indicated) is cloned behind the renilla luciferase in the dual luciferase reporter adenovirus. Cells were coinfected with the dual luciferase reporter and adenoviruses as indicated. The average of three independent experiments is shown in (**e**) ($p<0.0001$ (WT), NS=not significant, p=0.217 (Dicer1$^{-/-}$) and (**f**) (p=0.003 (B9), $p<0.0001$ (E7), $p<0.0001$ (E7 with tamoxifen treatment (+4'OH-T)).

Figure 6. Roquin binds to *ICOS* mRNA through its ROQ and Zinc finger domains. (**a,b**) Coimmunoprecipitation (Ppt) of Roquin detected by immunoblot (**a**) and endogenous *Icos* mRNA by RT-PCR (**b**) from protein extracts of T_H1 cells using a polyclonal anti-Roquin antibody. The average immunoprecipitated mouse *Icos* mRNA is displayed as percentage of input levels of three independent experiments (**b,** p=0.012 (asterisk)). (**c,f**) Representative RNA-immunoprecipitation with anti-GFP antibodies using protein extracts from HEK293 cells that were transfected with ICOS and GFP-tagged wild-type or deletion mutants of Roquin. *ICOS* mRNA levels are shown as percentage of input. (**d,e**) Representive plots of ICOS and Roquin (as Thy-1.1) expression (**d**) and mean fluorescence intensity of ICOS (**e**) in MEF cells sequentially transduced with retroviruses encoding for ICOS and the indicated Roquin proteins. One representative analysis out of three (**d**) or the average of three independent experiments is shown and analysed as above (**Fig. 2b,c**) (**e**, p=0.002 (asterisk), p= 0.001 (two asterisks), p=0.006 (bold asterisk)).

Figure 7. Roquin binds to *ICOS* mRNA with intrinsic preference for a specific region within the 3'UTR. (**a,b**) Electromobility shift assay with increasing amounts (pmol) of recombinant Roquin(1–441) protein, incubated with 1 pmol *in vitro* transcribed *ICOS* mRNA containing the 3'UTR (full-length) or lacking the 3'UTR (*ICOS* CDS) (**a,b**) or with *ICOS* mRNAs, in which the 3'UTR was progressively shortened from *ICOS*(1–900) to *ICOS*(1–700) (**b**). (**c,d**) Representative plot of ICOS and Roquin (as Thy-1.1.) expression (**c**) and mean fluorescence intensity of ICOS (**d**) in MEF cells sequentially transduced with retroviruses coding for Roquin and ICOS or ICOS with a progressively shortened 3'UTR. One representative analysis out of three (**c**) or the average ICOS expression in Thy1.1 high cells normalized to ICOS expression in Thy-1.1 negative cells of three independent experiments is shown (**d**, $p=0.015$ (one asterisk), $p<0.001$ (all two asterisks)).

Author contribution

E.G. performed most experiments, with the help of K.P.H., N.R. and assistance from C.W.. K.U.V. contributed some experiments and edited the manuscript. L.D. E.K. and X.W. established tools and provided advice. E.G. and V.H. planned the project together and V.H. supervised the experiments and wrote the manuscript.

Methods

Mice

Mice were obtained from Taconic farms, housed in a specific pathogen-free barrier facility and used in accordance with the Helmholtz Zentrum München institutional, state and federal guidelines at 6-12 weeks of age.

Cell culture and transfection

HEK293 cells and MEF cells were grown in DMEM with 10% FCS, 1000 U/ml penicillin-streptomycin and 10 mM HEPES. ES cells were grown in DMEM including 20% FCS, 2 mM L-glutamine, 100 U/ml penicillin-streptomycin, 1 mM sodium pyruvate, 0.1 mM non-essential amino acids, 0.1 mM ß-mercaptoethanol and 2000 U/ml LIF first on feeder cells and passaged twice on 0.1% gelatine. Peripheral $CD4^+$ T cells were isolated with CD4 Dynabeads (Invitrogen), kept in RPMI (10% FCS, 0.1 mM ß-mercaptoethanol, 100 U/ml penicillin-streptomycin, 10 mM HEPES) and stimulated for 36-48 h under T_H0-conditions on goat anti-hamster-IgG-coated surfaces with 0.1 μg/ml anti-CD3 and 1 μg/ml anti-CD28 or under T_H1-conditions by including anti-IL-4 (10 μg/ml) and IL-12 (10 ng/ml, R&D Systems) or under T_H2-conditions by including anti-IL-12 (3 μg/ml) and anti-IFNγ antibodies (5 μg/ml) as well as murine IL-4 containing supernatants from I3L6 cells (corresponding to 1000 U/ml recombinant IL-4). Beads stimulation was performed with tosyl-activated-M-450 beads (Invitrogen) coupled to anti-CD28 and anti-CD3. After stimulation for 48 h, cells were expanded in 10 U/ml recombinant human IL-2 (WHO, NIBSC).

Virus production

Type 5 replication-deficient adenoviruses were produced by transfection of adenoviral vectors into HEK293 cells and purified according to the manufacturers' instructions (Cell Biolabs). Retroviral supernatants were produced by calcium phosphate transfection of amphotropic packaging vectors and retroviral expression vectors in HEK293T cells. Supernatants were collected 72 h post transfection, filtered through 0.45 μm filters and used for spin-infections. Transduced cells were analyzed 3-4 days post-infection on a FACS Calibur device or sorted on a FACS ARIAII device (Becton Dickinson).

Adenoviral knockdown or ectopic protein expression

Adenoviral vectors with shRNAs (sh-control, tttttggccttttttagctg), (sh-scr control acaagatgaagagcaccaa), (sh-*Rc3h1,* cgcacagttacagagctcatt), (sh-*Cd4,* cacagctatcacggcctataa) or (sh-*Rck*, gccaagaactatgtctttata) placed under the control of a U6 promoter and coexpressed with *pgk* promoter-driven EGFP were

purchased (Sirion Biotech). The adenoviral expression vector was created by assembling the artificial CAG promoter in front of a Gateway cassette followed by a poly-(A) signal from the bovine growth hormone in the pAd-Pl vector (Invitrogen), into which GFP–Roquin was inserted via lambda-recombination from an Entry vector.

Luciferase assay

MEF cells were plated on 12-well plates and infected with adenoviruses. After two days the dual-luciferase reporter assay (Promega) was performed. Cells were lysed in 150 µl lysis-buffer, lysates were cleared by centrifugation and 20 µl supernatant were analyzed.

Real-time PCR

RNA from cells or immunoprecipitates was isolated with Trizol (Sigma) or MirVana kit (Ambion), respectively. After reverse transcription with the Quantitect kit (Qiagen,) qPCR assays used the following primers and universal probes (Roche, http://www.roche-applied-science.com/sis/rtpcr/upl/ezhome.html): mIcos F1: cggcagtcaacacaaacaa, R1: tcaggggaactagtccatgc, probe: #6; hICOS F2: ggatgcatacttatttgttggctta, R2: tgtattcaccgttagggtcgt, probe #47; mRc3h1 F3: gagacagcaccttaccagca, R3: gacaaagcgggacacacat, probe #22; mRc3h2 F4: ttgtcagccaccgaatgac, R4: ttcaaatgaccacaaggttcc, probe# 98. Normalizations used Hprt1 F1: tcctcctcagaccgctttt, R1: cctggttcatcatcgctaatc, probe: #95 or Ywhaz F2: cgctaataatgcagttactgagaga, R2: ttggaaggccggttaatttt, probe #2 (**Fig. 1f,g**). Primers-probe-sets were efficiency-tested to allow efficiency-correction. MiRNA expression was determined and normalized to U6 using the TaqMan microRNA Reverse Transcription kit and stem-loop primers specific for miR-101, miR-328, miR-196a miR-214, miR-155, miR-181 and U6 (Applied Biosystems). Quantitative PCRs were performed on a LightCycler 480II.

Confocal microscopy

HEK293 cells were transfected with FuGENE reagent (Roche), seeded on glass cover slips and stressed for 1 h with 0.5 mM sodium arsenite (Sigma) at 37°C.

Diagnostica glass cover slips were coated with 0.01% (w/v) poly-L lysine and then with anti-CD3 (2.5 μg/ml) and anti-CD28 (5 μg/ml) before adding T cells in 50 μl. Cells were fixed with 4% paraformaldehyde and washed three times in PBS + 0.5% NP-40, 0.01% NaN_3, 10% FCS. Anti-p70 S6 kinase α, anti-G3BP (Santa Cruz sc-8418 or sc-81940) and anti-Rck (Bethyl A300-461A) or anti-FMRP antibodies were used for staining in combination with Cy5- and Cy3-coupled secondary antibodies (Jackson). Pictures were captured on a Leica DM IRBE microscope and analyzed with LCS Lite software.

Coimmunoprecipitation of Roquin associated *Icos* mRNA or proteins

Coimmunoprecipitation of Roquin-associated RNA or protein was performed as previously described [36]. Briefly, $2x10^8$ T cells or $1x10^7$ HEK293 cells were lysed on ice in 2 ml lysis-buffer (20 mM Tris pH 7.5, 150 mM NaCl, 0.25% NP-40, 1.5 mM $MgCl_2$, protease inhibitor mix without EDTA (Roche) and 1 mM DTT). Lysates were passaged through a 26G needle, shock frozen, thawn and cleared by centrifugation. Anti-Roquin or -GFP antibodies bound to protein G magnetic beads (Invitrogen) were incubated with lysates in the presence of 20 U RNasin at 4°C for 4 h. The beads were washed twice with lysis-buffer and two to four times with lysis-buffer containing 300 mM NaCl, 0.5% NP-40, 2.5 mM $MgCl_2$.

Purification of Roquin protein

Roquin(1–441) was expressed from petM11 in bacteria, purified by His-tag chromatography (GE Healthcare) and desalted via PD10 gel filtration (GE Healthcare).

***In vitro* RNA transcription**

For *in vitro* transcription pDest17 constructs were linearized by restriction. *In vitro* transcription of mRNA was carried out with the mMessage mMachine T7 transcription kit according to the manufacturers' instructions (Ambion) and RNA was purified with the RNeasy Kit (Qiagen).

Mass spectrometry

For the identification of coimmunoprecipitated proteins SDS-PAGE slices were analyzed using an LC-MS/MS approach with an LTQ Orbitrap XL mass spectrometer coupled to an Ultimate 3000 Nano-HPLC. All MS/MS spectra were then analyzed with the Mascot search engine against the uniref100_mouse fasta database. Protein identifications were accepted if they could be established at greater than 95% probability and contained at least 2 identified peptides.

Electromobility shift assays

Electromobility shift assays were performed on native 0.75% agarose gels, stained with ethidium bromide. Recombinant protein (5 – 160 pmol) was incubated with *ICOS* mRNA (0.6 or 1 pmol) for 20 min on ice (150 mM KCl, 50 mM Tris/HCl pH 7.4, 1 mM $MgCl_2$, 1 mM EDTA, 1 mM DTT) and then adjusted to 16% glycerol.

References

1. Yu, D. et al. Roquin represses autoimmunity by limiting inducible T-cell co-stimulator messenger RNA. *Nature* **450**, 299-303 (2007).
2. Vinuesa, C.G. et al. A RING-type ubiquitin ligase family member required to repress follicular helper T cells and autoimmunity. *Nature* **435**, 452-8 (2005).
3. Anderson, P., Phillips, K., Stoecklin, G. & Kedersha, N. Post-transcriptional regulation of proinflammatory proteins. *J Leukoc Biol* **76**, 42-7 (2004).
4. Hao, S. & Baltimore, D. The stability of mRNA influences the temporal order of the induction of genes encoding inflammatory molecules. *Nat Immunol* **10**, 281-8 (2009).
5. Hoefig, K.P. & Heissmeyer, V. MicroRNAs grow up in the immune system. *Curr Opin Immunol* **20**, 281-7 (2008).
6. Stefl, R., Skrisovska, L. & Allain, F.H. RNA sequence- and shape-dependent recognition by proteins in the ribonucleoprotein particle. *EMBO Rep* **6**, 33-8 (2005).
7. Jing, Q. et al. Involvement of microRNA in AU-rich element-mediated mRNA instability. *Cell* **120**, 623-34 (2005).
8. Kedde, M. et al. RNA-binding protein Dnd1 inhibits microRNA access to target mRNA. *Cell* **131**, 1273-86 (2007).
9. Vasudevan, S. & Steitz, J.A. AU-rich-element-mediated upregulation of translation by FXR1 and Argonaute 2. *Cell* **128**, 1105-18 (2007).

10. Tan, A.H., Wong, S.C. & Lam, K.P. Regulation of mouse inducible costimulator (ICOS) expression by Fyn-NFATc2 and ERK signaling in T cells. *J Biol Chem* **281**, 28666-78 (2006).
11. Bossaller, L. et al. ICOS deficiency is associated with a severe reduction of CXCR5+CD4 germinal center Th cells. *J Immunol* **177**, 4927-32 (2006).
12. Dong, C. et al. ICOS co-stimulatory receptor is essential for T-cell activation and function. *Nature* **409**, 97-101 (2001).
13. Dong, C., Temann, U.A. & Flavell, R.A. Cutting edge: critical role of inducible costimulator in germinal center reactions. *J Immunol* **166**, 3659-62 (2001).
14. McAdam, A.J. et al. Mouse inducible costimulatory molecule (ICOS) expression is enhanced by CD28 costimulation and regulates differentiation of CD4+ T cells. *J Immunol* **165**, 5035-40 (2000).
15. Tafuri, A. et al. ICOS is essential for effective T-helper-cell responses. *Nature* **409**, 105-9 (2001).
16. Linterman, M.A. et al. Follicular helper T cells are required for systemic autoimmunity. *J Exp Med* **206**, 561-76 (2009).
17. Wan, Y.Y. et al. Transgenic expression of the coxsackie/adenovirus receptor enables adenoviral-mediated gene delivery in naive T cells. *Proc Natl Acad Sci U S A* **97**, 13784-9 (2000).
18. Oberdoerffer, P. et al. Efficiency of RNA interference in the mouse hematopoietic system varies between cell types and developmental stages. *Mol Cell Biol* **25**, 3896-905 (2005).
19. Heissmeyer, V., Ansel, K.M. & Rao, A. A plague of autoantibodies. *Nat Immunol* **6**, 642-4 (2005).
20. Chu, C.Y. & Rana, T.M. Translation repression in human cells by microRNA-induced gene silencing requires RCK/p54. *PLoS Biol* **4**, e210 (2006).
21. Didiot, M.C., Subramanian, M., Flatter, E., Mandel, J.L. & Moine, H. Cells lacking the fragile X mental retardation protein (FMRP) have normal RISC activity but exhibit altered stress granule assembly. *Mol Biol Cell* **20**, 428-37 (2009).
22. Mazroui, R. et al. Trapping of messenger RNA by Fragile X Mental Retardation protein into cytoplasmic granules induces translation repression. *Hum Mol Genet* **11**, 3007-17 (2002).
23. Franks, T.M. & Lykke-Andersen, J. The control of mRNA decapping and P-body formation. *Mol Cell* **32**, 605-15 (2008).
24. Michelitsch, M.D. & Weissman, J.S. A census of glutamine/asparagine-rich regions: implications for their conserved function and the prediction of novel prions. *Proc Natl Acad Sci U S A* **97**, 11910-5 (2000).
25. Reijns, M.A., Alexander, R.D., Spiller, M.P. & Beggs, J.D. A role for Q/N-rich aggregation-prone regions in P-body localization. *J Cell Sci* **121**, 2463-72 (2008).
26. Gilks, N. et al. Stress granule assembly is mediated by prion-like aggregation of TIA-1. *Mol Biol Cell* **15**, 5383-98 (2004).

27. Parameswaran, P. et al. Six RNA viruses and forty-one hosts: viral small RNAs and modulation of small RNA repertoires in vertebrate and invertebrate systems. *PLoS Pathog* **6**, e1000764 (2010).
28. Yekta, S., Tabin, C.J. & Bartel, D.P. MicroRNAs in the Hox network: an apparent link to posterior prevalence. *Nat Rev Genet* **9**, 789-96 (2008).
29. Su, H., Trombly, M.I., Chen, J. & Wang, X. Essential and overlapping functions for mammalian Argonautes in microRNA silencing. *Genes Dev* **23**, 304-17 (2009).
30. Athanasopoulos, V. et al. The ROQUIN family of proteins localizes to stress granules via the ROQ domain and binds target mRNAs. *Febs J* **277**, 2109-27 (2010).
31. Scheu, S. et al. Activation of the integrated stress response during T helper cell differentiation. *Nat Immunol* **7**, 644-51 (2006).
32. Cougot, N., van Dijk, E., Babajko, S. & Seraphin, B. 'Cap-tabolism'. *Trends Biochem Sci* **29**, 436-44 (2004).
33. Eulalio, A., Behm-Ansmant, I. & Izaurralde, E. P bodies: at the crossroads of post-transcriptional pathways. *Nat Rev Mol Cell Biol* **8**, 9-22 (2007).
34. Parker, R. & Sheth, U. P bodies and the control of mRNA translation and degradation. *Mol Cell* **25**, 635-46 (2007).
35. Lunde, B.M., Moore, C. & Varani, G. RNA-binding proteins: modular design for efficient function. *Nat Rev Mol Cell Biol* **8**, 479-90 (2007).
36. Weinmann, L. et al. Importin 8 is a gene silencing factor that targets argonaute proteins to distinct mRNAs. *Cell* **136**, 496-507 (2009).

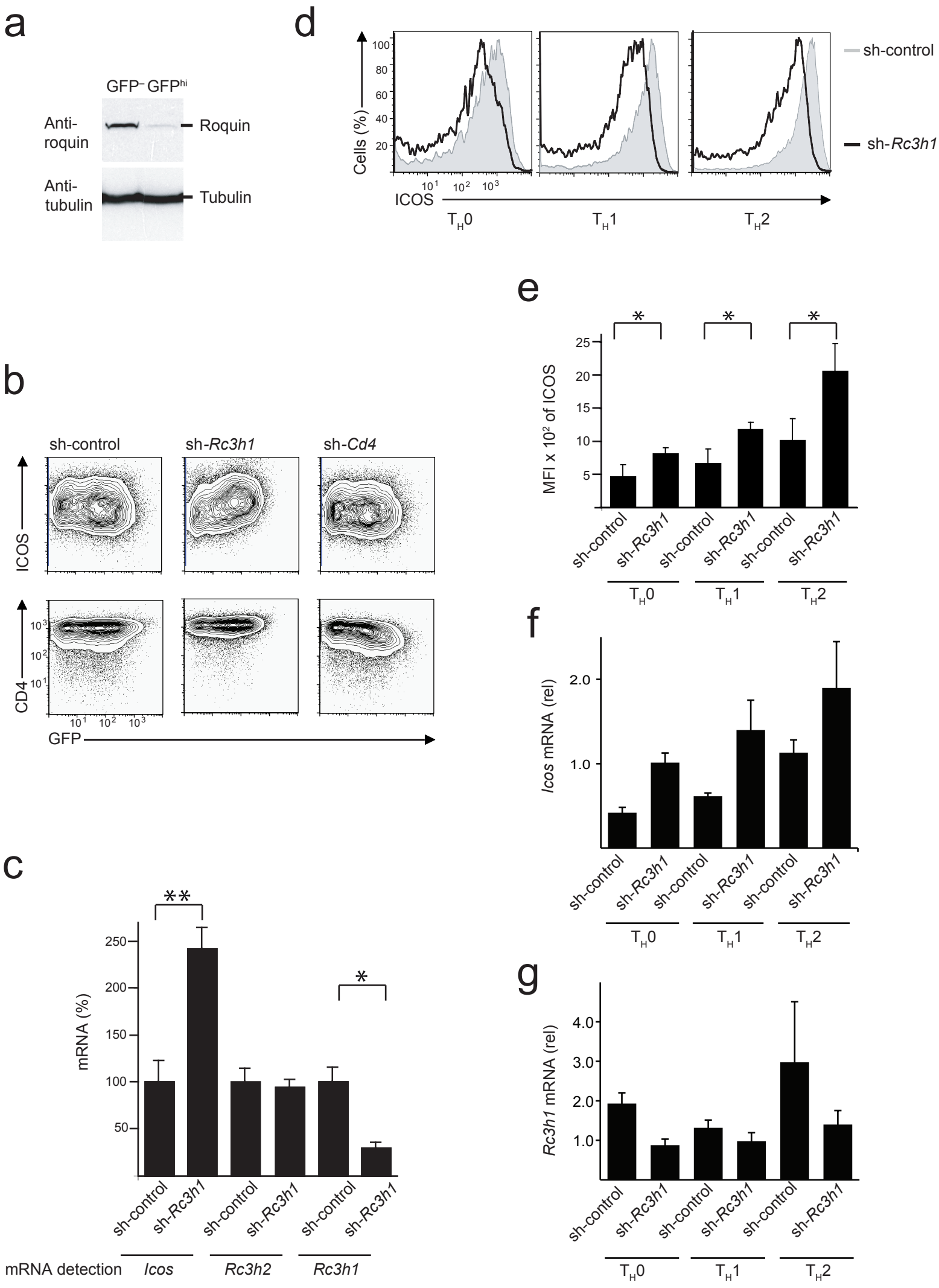

Glasmacher Figure 1

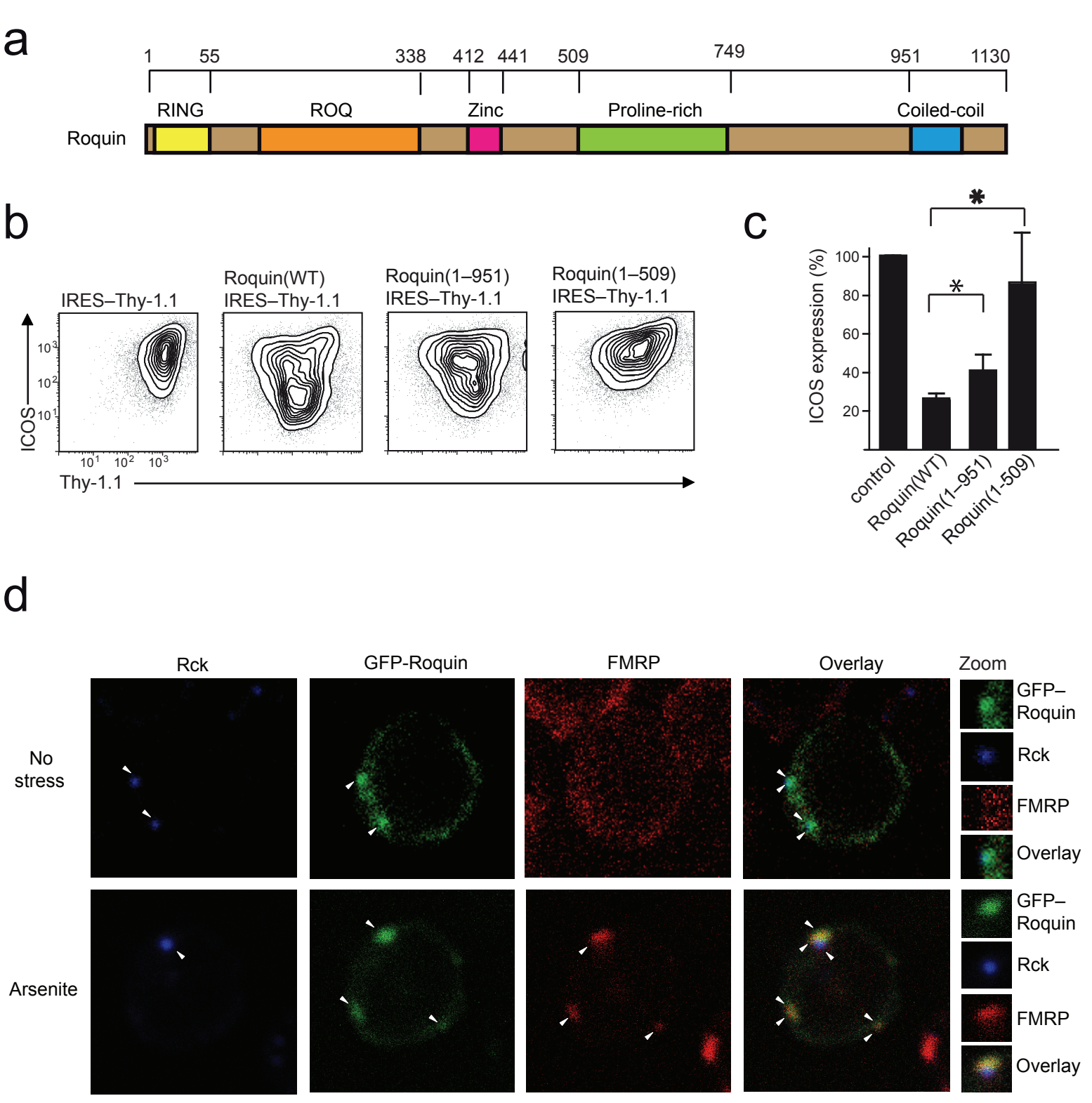

Glasmacher Figure 2

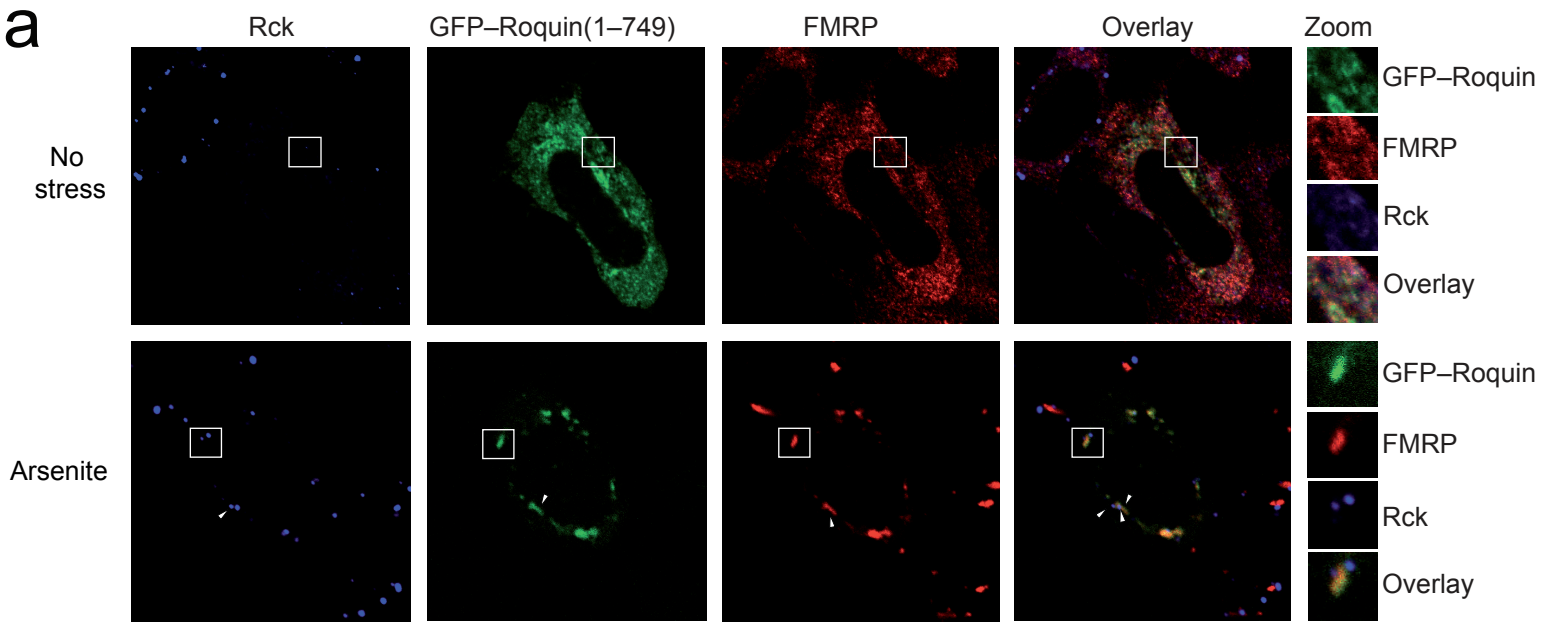

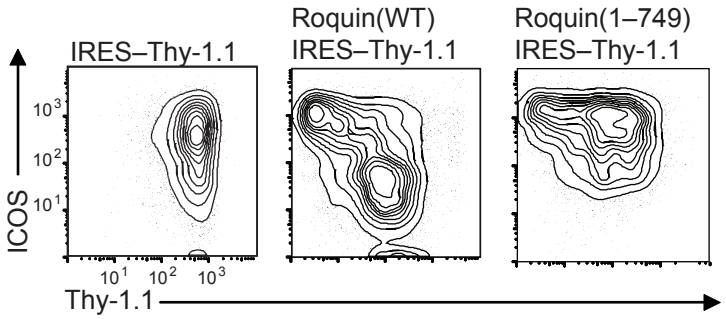

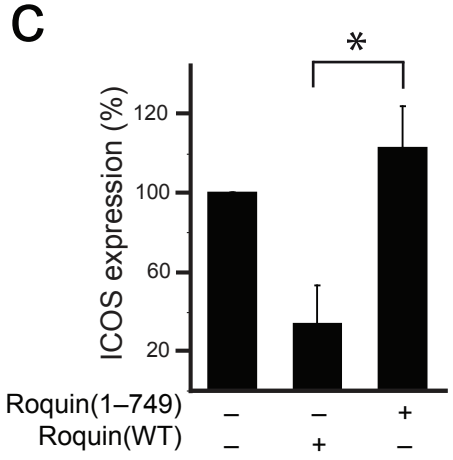

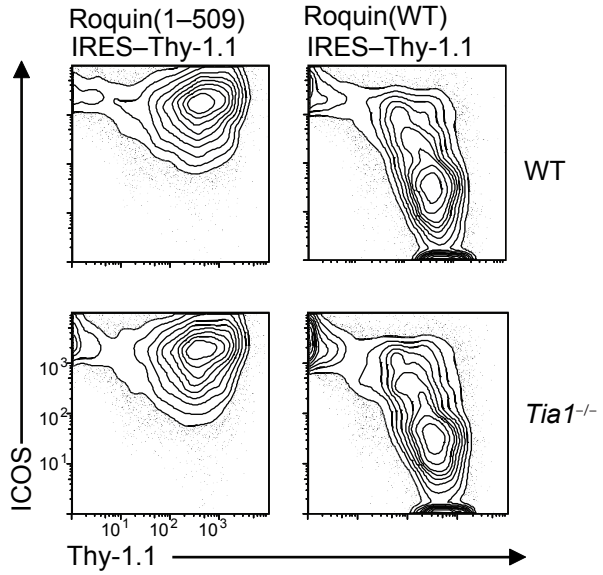

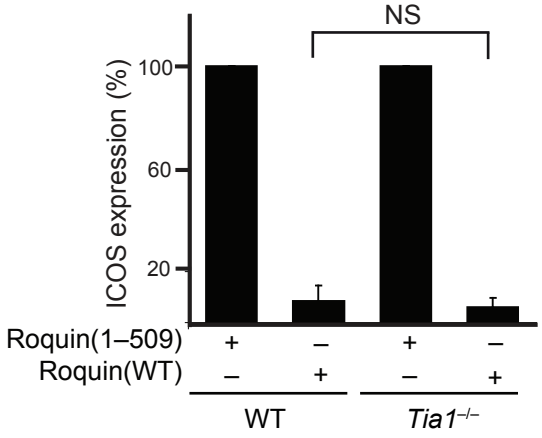

Glasmacher Figure 3

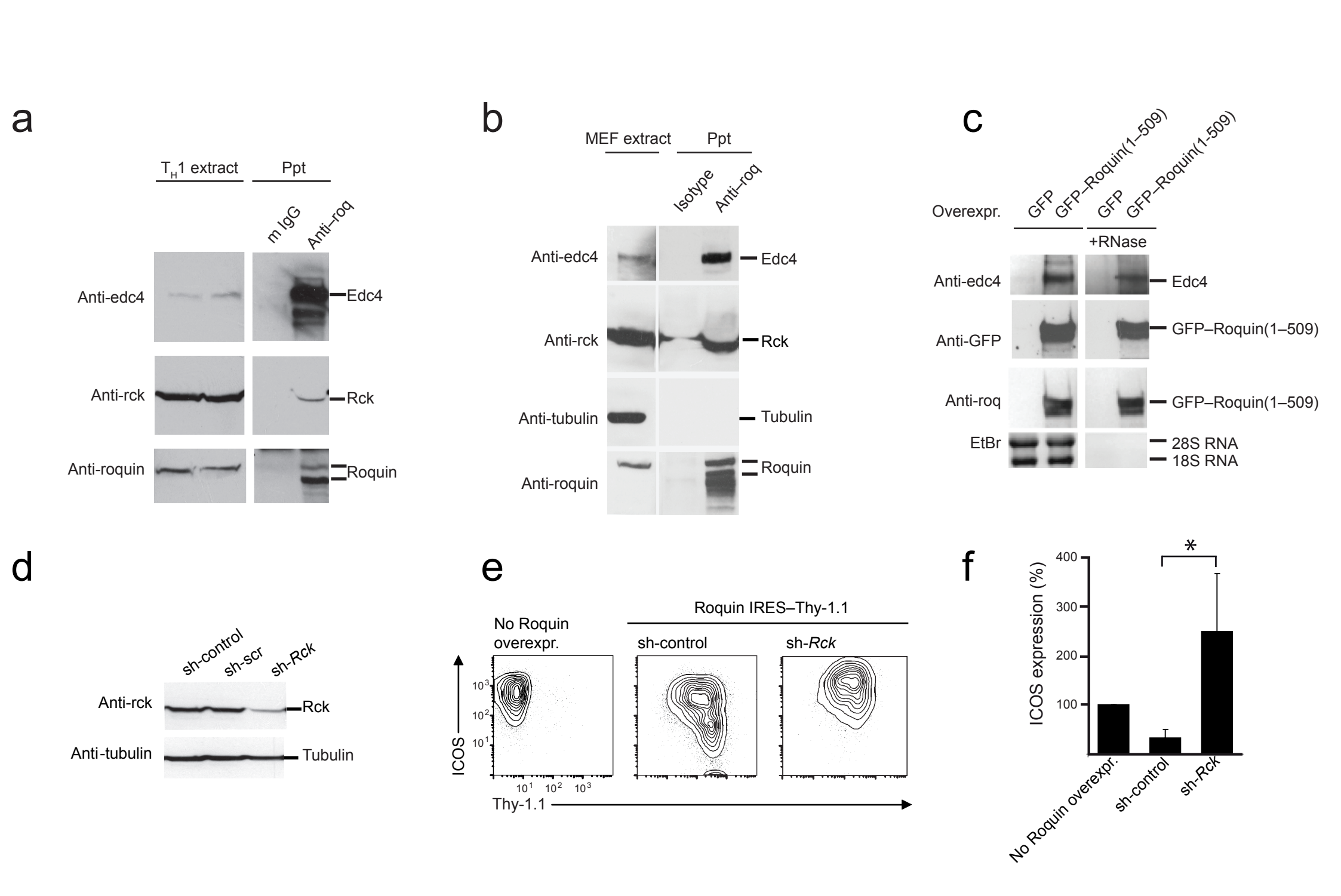

Glasmacher Figure 4

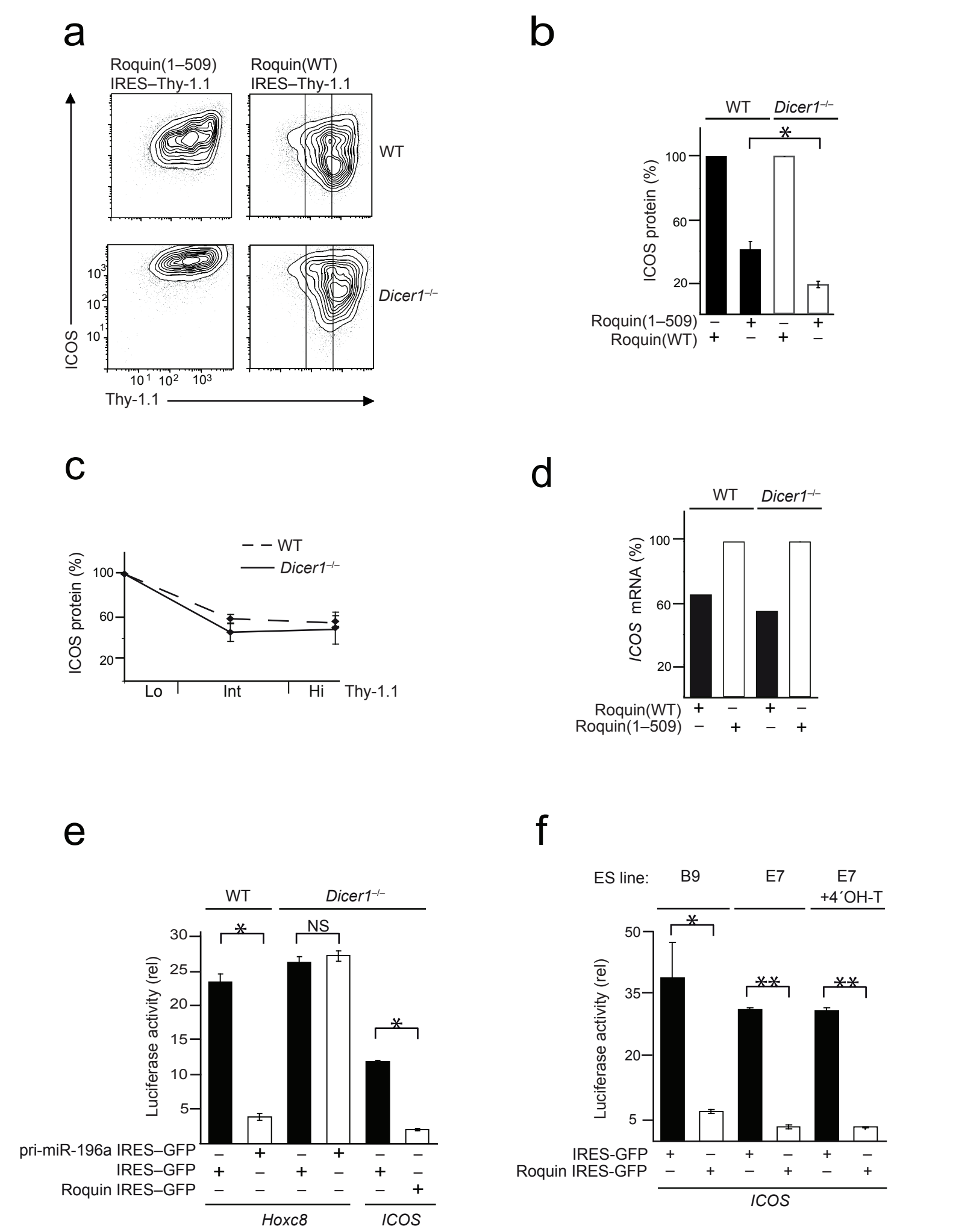

Glasmacher Figure 5

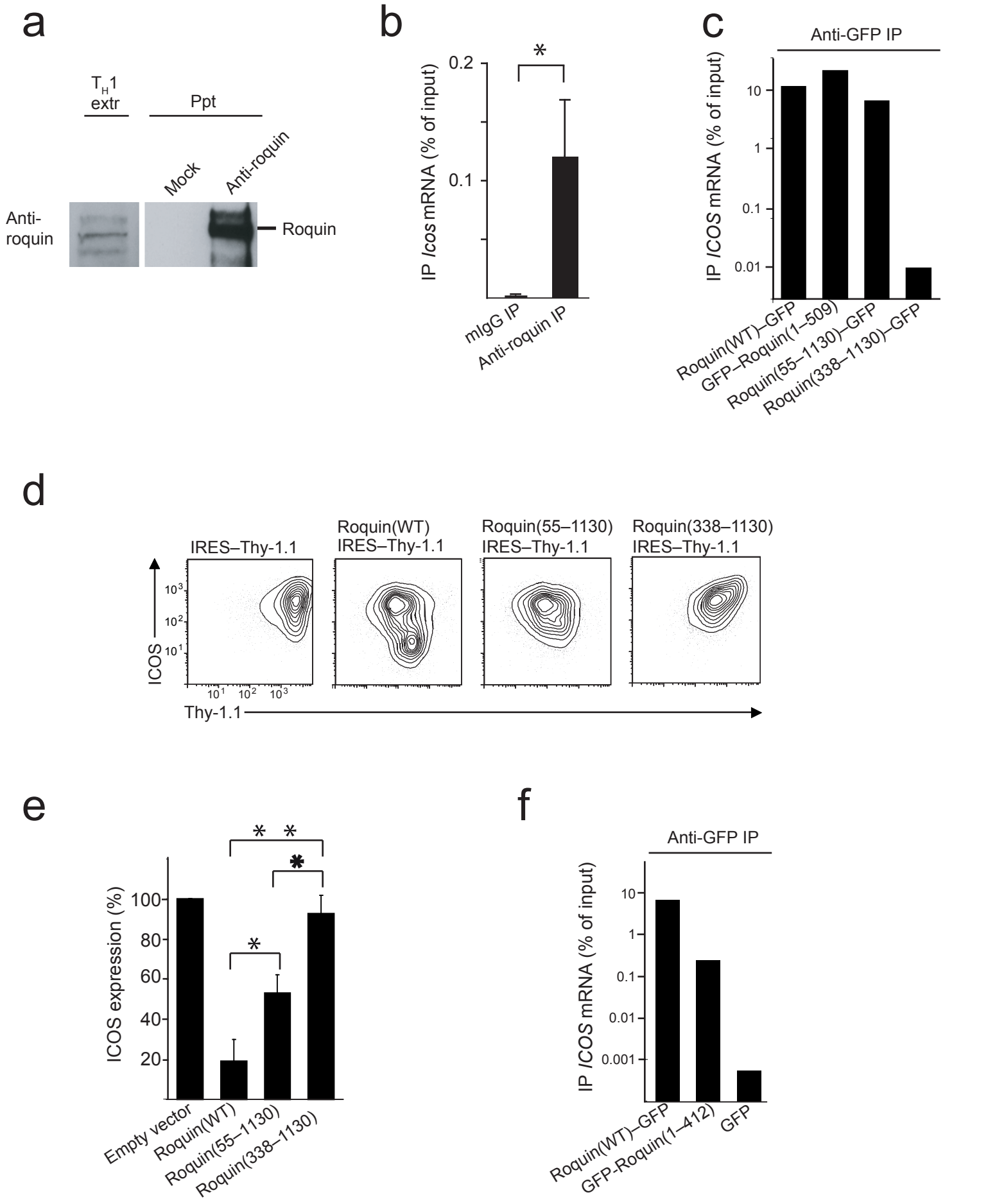

Glasmacher Figure 6

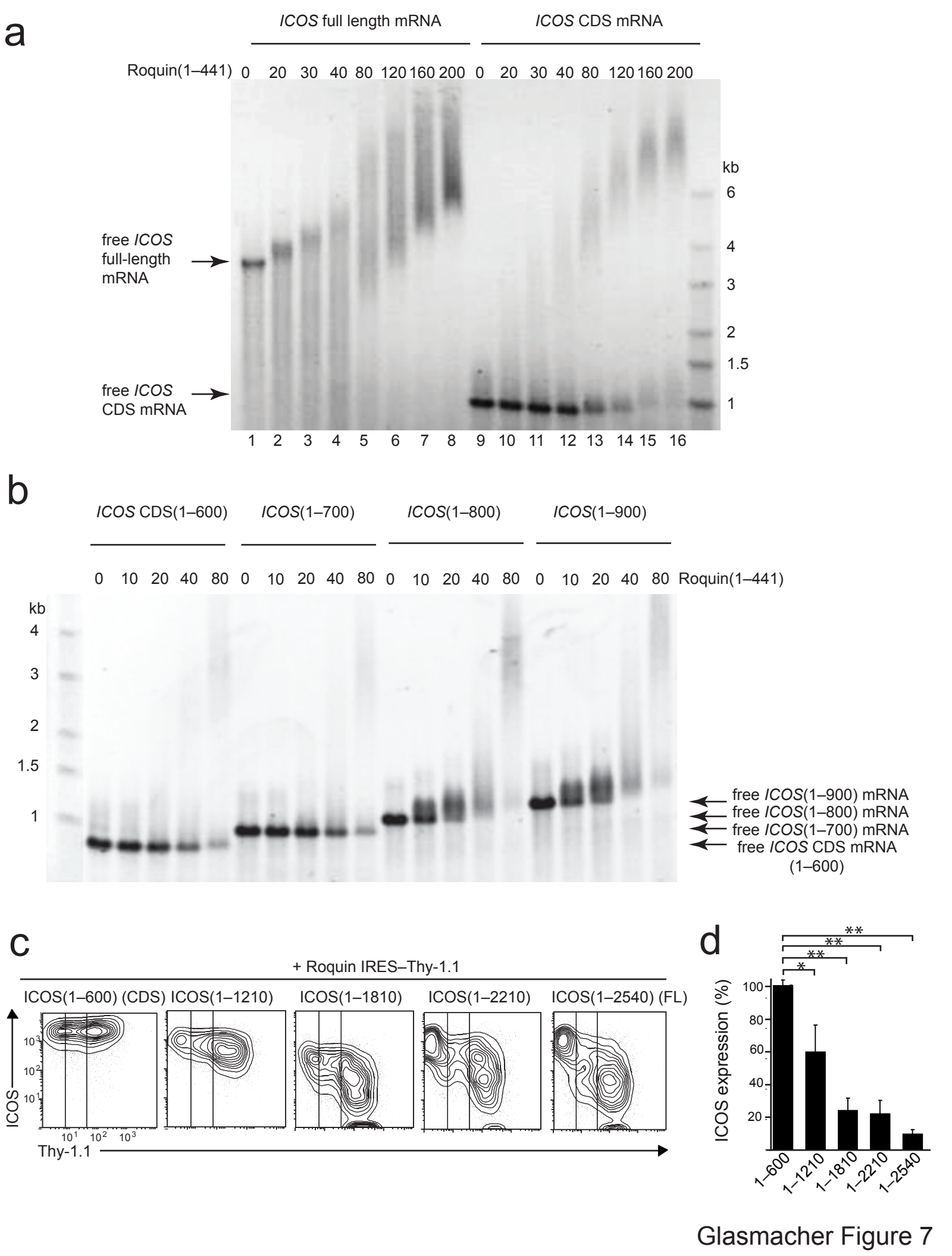

Glasmacher Figure 7